



SUPPRESSION EFFECTIVENESS OF WATER MIST ON ACCIDENTAL AIRCRAFT FIRES

Akira Yoshida*, Wataru Ebina*, Toichiro Okawa*

*Tokyo Denki University

Keywords: fire suppression, water mist, premixed flame, flame speed, CHEMKIN

Abstract

Water mist is expected to have physical and chemical effects on the laminar flame speeds. In the present study, the effect of water mist on flame speed of propane-air premixed flames was investigated both experimentally and numerically. Experiments were performed using a single-jet-plate configuration and the OPPDIF program in CHEMKIN package was used in the numerical simulation. To include the evaporation process of water mist in simulation, evaporation process was assumed to follow the Arrhenius law. The contribution of water mist on flame speeds was separated into the dilution and chemical effects of water vapor, and the thermal effect of liquid water which includes the heat of evaporation. The most effective is the sensible heat of water vapor, followed by the heat of evaporation. The chemical effect is relatively small but cannot be neglected. When the water mist is added, the flame temperature decreases due to thermal effect which reduces the rates of chemical reactions involving the radicals such as O and H, which have the positive sensitivity of flame speed. Furthermore, three-body chain-terminating reactions involving H₂O are enhanced. These reactions have large negative sensitivity of flame speed due to high chaperon efficiency of water vapor.

1 Introduction

Water mist is a favorable substitute for typical halogenated hydrocarbon fire suppressants, e.g. Halon 1301 (CF₃Br) and Halon 1211 (CF₂ClBr), because water mist is ubiquitous, inexpensive, non-electrically conductive and environmentally acceptable and also is fairly effective to

suppress fires and to mitigate explosions [1-4]. Adding water mist in a reactive mixture is known to cause significant changes in flame properties by three following mechanisms; (a) thermal effect due to the absorption of the heat, (b) dilution effect caused by the reduction in reactants concentration, and (c) chemical effect owing to the activity of water vapor that may alter some reaction paths. Fine water mist enhances these effects due to significant increase in the surface area available for heat absorption and evaporation. Those three mechanisms are concomitant and closely linked with each other. In addition, the flame stretch also affects the flame properties and extinguishment process. However, few studies exist in the literature relating to the effect of water mist on the stretched flame from the point of view of fire suppression and explosion mitigation.

The effectiveness of gaseous water vapor as a fire suppressant has also been long recognized. The influences of gaseous water vapor on the laminar flame speed of methane flames were investigated [5], and the numerically predicted reduction in flame speed was in good agreement with the experiments. In addition, the chemical effect of water vapor on the combustion reactions of H₂-CH₄-Air mixtures was found to be small but not negligible [6]. Effects of elevated temperatures and pressures on the laminar flame speed of H₂-O₂-water vapor system were studied both experimentally and computationally [7], and a significant reduction of the flame speed was found by addition of water vapor.

Liquid water has a more favorable thermal property for fire suppression than gaseous water vapor, because it has a high latent heat of

evaporation and can absorb a significant quantity of heat from flames. Therefore, water mist was found to be more effective in reducing the flame speed of methane-air flames than other gaseous thermal agents (N_2 and CF_4) or chemical agents (CF_3Br), and also more effective than the same mass of gaseous water vapor [8]. Furthermore, the flame speeds of propane-air premixed flame stabilized in the stagnation flow field were measured under the influence of water mist [9] and the dependence of flame speed on stretch rate was found to change from positive to negative by adding water mist. In the diverging flow field, the mist droplets accumulate around the stagnation stream line due to the Stokes number effect; mist droplets cannot follow the large radial acceleration which occurs in the stagnation flow field.

Laminar flame speed is a fundamental property of a flammable gaseous mixture describing the overall reaction rate, heat release, and heat and mass transport in the flame and as such many efforts have been devoted to measure or predict the precise laminar flame speeds of various kinds of fuels. For the flame speed measurement, the counterflow, opposed-jet technique is well documented [10-15], and has been traditionally implemented with the use of twin-opposed-nozzle or single-jet-plate configurations. In a twin-flame or single-flame configuration, the velocity minimum is identified in the velocity profile as a reference upstream flame speed S_L and the velocity gradient a ahead of the minimum point is identified as the stretch rate K ($= a$ for an axisymmetric flame) experienced by the flame. The unstretched laminar flame speed S_L^0 is obtained by systematically determining the dependence of the reference flame speed S_L on the stretch rate K and extrapolating S_L to zero K .

The reduction in laminar flame speed is frequently used as an indicator of the fire suppression effectiveness of an inhibiting agent [16-18]. The impact of gaseous water vapor or liquid water mist on stretched laminar flame has been the subject of a relatively limited number of studies. In the present study, the effects of water mist on the laminar flame speeds of propane-air mixtures were investigated both

experimentally and numerically. In the experiments, stretched laminar premixed flames were established in the stagnation flow field produced by a mixture flow emerging from a nozzle. The unstretched laminar flame speed S_L^0 was obtained by a nonlinear extrapolation to zero stretch. The effect of water mist on flame structure and flame speed was also simulated numerically by using OPPDIF program in CHEMKIN package, modified to include the evaporation process, which was assumed to be a chemical reaction.

2 Experiments

A single-jet-plate configuration was adopted in the present study for the precise measurements of laminar flame speeds of propane/air mixtures with and without water mist.

2.1 Experimental Apparatus

Hitherto, a twin-flame [10-14] or a single-flame [15] has been used for the determination of laminar flame speeds and stretch rates at extinguishment of H_2 and C_1-C_3 hydrocarbon fuels. In the present study, experiments were performed in the single-jet-plate configuration for atmospheric propane/air flames at different equivalence ratios with and without water mist in the mixture. The details of experimental apparatus have been described in Ref. 9. In brief, the single-jet-plate configuration included impingement of mixture flow from a contoured nozzle on a stainless steel stagnation plate. The inside diameter of the nozzle exit was 45 mm. The mixture flow was surrounded by a shroud flow of air to protect from the disturbances caused by the entrainment of surrounding air. Propane was used as a fuel throughout. Water mist diameters and their distributions were measured by a phase Doppler particle analyzer (PDPA) and the flow velocity by a laser Doppler velocimeter (LDV). For PDPA and LDV measurements, the mixture flow should be seeded with light scattering particles. For the case without water mist, the mixture flow was seeded with aluminum oxide (Al_2O_3) particles of a nominal diameter of 1 μm , generated by a fan-stirred particle generator. When the water

mist was added to the mixture flow, the water mist itself played a role of light scattering particles. To generate fine water mist, 6 piezoelectric atomizers were used, which could be operated separately. The amount of water mist added to the mixture was adjusted by the number of atomizers activated. The number mean diameter of water mist droplets D_{10} was 11.5 μm and the Sauter mean diameter D_{32} was 18.4 μm with a wide range of size distribution ranging from 1 μm to 60 μm .

2.2 Unstretched laminar flame speed without water mist, S_L^0

The experimental conditions were limited within the range of equivalence ratio, $0.8 < \phi < 1.3$, because, when $\phi > 1.4$, the cellular instability appeared at small velocity gradient a for large separation distance L and small flow velocity u , and when $\phi < 0.7$, the flame was deformed significantly and was not stationary at small a .

The velocity profile along the stagnation stream line can be considered to be the superposition of the effects of the flame and the stagnation flow field. When approaching the flame zone, the velocity decreases almost linearly with the distance from the stagnation plate z . The velocity gradient $a = du/dz$ was obtained from the velocity profile along the stagnation stream line. The flame stretch rate K coincides with the velocity gradient a for an axisymmetric flame. The velocity abruptly increases in the flame zone due to thermal expansion, and then decreases again towards the stagnation plate. The velocity at the point of initial temperature rise is the point where the curve starts to depart from the descending line due to thermal expansion, and the minimum point was defined as a reference upstream flame speed of a stretched flame S_L , similarly to previous investigations by Law and co-workers [10-15]. The unstretched laminar flame speed S_L^0 can be subsequently determined by systematically extrapolating S_L to zero K . By increasing the nozzle exit velocities, K increases, the flames are pushed toward the stagnation plate, and extinguishment is eventually obtained when a critical value K_{ext} is reached.

3 Numerical Simulations

The OPPDIF program in the CHEMKIN package was utilized to simulate the flame structure and the flame speed of stretched, adiabatic, laminar propane-air premixed flames stabilized in the stagnation flow field. The flame speeds estimated by CHEMKIN depend on the reaction mechanism adopted. The present chemical kinetic models for propane oxidization were based on the San Diego mechanism [19] and that proposed by Davis, Law and Wang [20]. In the San Diego mechanism, 46 chemical species and 235 elementary reactions are considered, whereas 71 species and 469 reactions are included in the DLW mechanism.

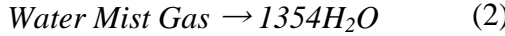
As the reference, the flame structure and the flame speed were calculated for the case without water mist, which hereafter is designated as $\langle O \rangle$. To highlight the effect of latent heat of evaporation of water, we first calculated the effects of gaseous water vapor on the structure and flame speed, neglecting the evaporation process. In this calculation, the added water vapor was assumed to be a virtual species, hereafter designated as $\langle V \rangle$, to investigate the effects of water vapor dilution on combustion chemistry. This virtual species was assigned the same molecular structure and the same thermodynamic and transport properties as water vapor. This virtual species however did not participate in the elementary reactions of the kinetic mechanism. Thereby, numerical calculations conducted with virtual species highlight only the dilution and thermal effects of water vapor. Then, the water vapor was assumed to participate in elementary chain branching, carrying and terminating reactions. The chain terminating reaction occurs through three-body collisions, in which the chaperon efficiency of H_2O is important. This case was designated as $\langle R \rangle$.

Finally, the latent heat of evaporation was included in the detailed kinetic mechanism. To include the phase change of water in the OPPDIF program, we assumed the liquid water mist to be an imaginary ideal gas, following the model proposed by Takahashi and Katta [21]. This imaginary gas was identified as the water mist gas. The conversion of this water mist gas

into gaseous water vapor was treated chemically as an Arrhenius reaction,

$$k = A \exp(-E/RT) \quad (1)$$

where A is the pre-exponential factor and E the activation energy. Thereby, the evaporation process is described by a chemical reaction,



The thermodynamic data of water mist gas was obtained by scaling the corresponding data of liquid water with the ratio of molecular weights. Activation energy, E and pre-exponential factor, A should depend on the evaporation process, i.e. the water mist mass loading and the mist diameter. In Ref. 21, these two parameters were obtained while calibrating the global reaction based on the criterion that water should fully evaporate by the time when the temperature reaches $T_{ev} = 500$ K. It was found that the increase of T_{ev} from 500 K to 1500 K induced no significant changes in the flame structure and flame speeds [22], and therefore $T_{ev} = 500$ K was assumed throughout the present study. Since liquid water is actually getting converted into H_2O vapor, latent heat of evaporation is automatically included. Thus, we can consider the effects of expansion, latent heat and chemical kinetics of water mist on laminar flame speed. This case was designated as <WMG>.

4 Results and Discussion

Numerical simulation was compared with

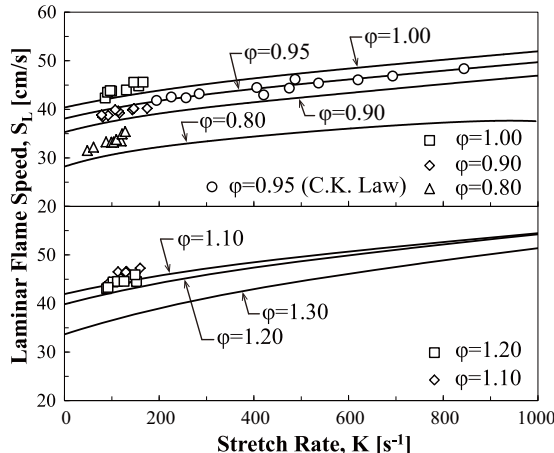


Fig. 1 Effect of stretch rate on laminar flame speeds; (a) Lean flames, (b) Rich flames.

experiments to highlight the fire suppression effectiveness of the water mist, and the suppression mechanism was deduced in the present study. In the first phase, the validity of the kinetic mechanism adopted in the simulation was checked by the comparison with existing data base of laminar flame speeds and also with the data obtained in the present study.

4.1 Laminar Flame Speeds without Water Mist

Laminar flame speed, S_L , is shown in Figs. 1a and 1b for lean and rich sides, respectively. Present experimental data and calculated values are concurrently presented in both figures. Calculated values are in fairly good agreement with experiments, indicating the nonlinear dependence of flame speed on stretch rate. Experimental data for $\phi = 0.95$ [11] are also shown in Fig. 1a and are in good agreement with the present study. Noteworthy is that the laminar flame speed increases with the stretch rate for all equivalence ratios tested.

Nonlinear extrapolations in Figs. 1a and 1b to $K = 0$ yield the laminar flame speeds without stretch S_L^0 . Figure 2 shows S_L^0 as a function of the equivalence ratio ϕ , in which the present experimental data are compared with numerically calculated values using different chemical kinetic mechanisms and with previous experiments using the counterflow configuration [14] and the flat flame burner [23]. The calculated values can be compared fairly

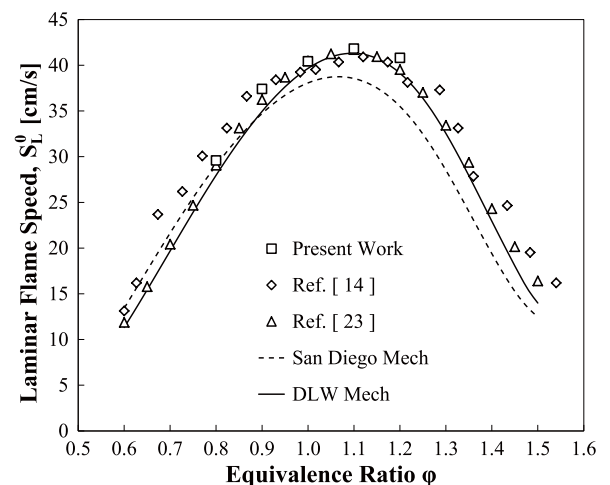


Fig. 2 Unstretched laminar flame speeds without water mist.

well with experimental data of Refs. 14 and 23, except for the lean side where the data obtained by the counterflow configuration are slightly higher than those obtained by the flat flame burner. However, the difference is considered within the experimental error. Although the present experiment is limited within the range of equivalence ratio of 0.8 and 1.3, the data are generally in reasonably good agreement with those of Refs. 14 and 23, in spite of the fact that the laminar flame speeds were determined by independent methodologies. The calculated data obtained by adopting the San Diego mechanism are close to the experimental data only on the lean side, whereas on the rich side the calculation predicts lower flame speeds. The DLW mechanism yields a better agreement with the experimental data, although the prediction slightly underestimates the flame speed on the lean side. Hereafter, the DLW mechanism is used to calculate the laminar flame speeds under the influence of water mist.

4.2 Laminar Flame Speeds with Water Mist

Evaporation process was modeled by a chemical reaction with an Arrhenius expression, where the Arrhenius parameters were determined by assuming the evaporation temperature T_{ev} , which was rather arbitrary.

4.2.1 Influence of T_{ev} on flame structure

The determination of the evaporation temperature T_{ev} is rather arbitrary and should be relied on the experimental data. Unfortunately, due to the lack of such data, parametric study on

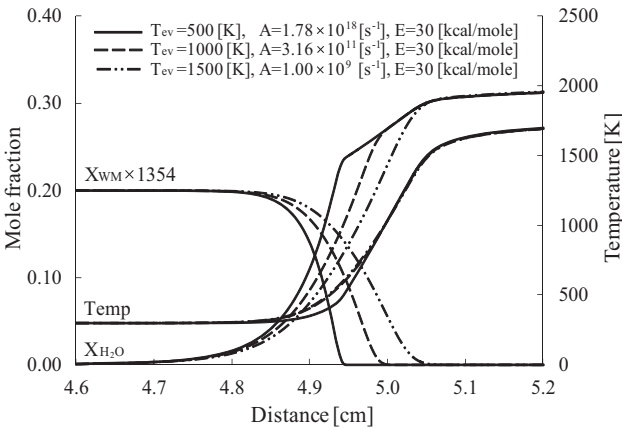


Fig. 3 Effect of T_{ev} on temperature distributions and evaporation processes for $\langle WM \rangle$, and $1354X_{wm} = 0.20$.

the activation energy, E and the pre-exponential factor, A was carried out. Figure 3 shows the evaporation process of water mist and resulting temperature distributions. Mole fraction of water mist added, X_{WM} was determined so that the mole fraction of water vapor, X_{H2O} is 0.20, when the water mist evaporates completely. With increase of the evaporation temperature, T_{ev} by adjusting the activation energy, E and the pre-exponential factor, A , the evaporation zone extends deeply into the flame zone. However, the temperature distribution is not affected significantly by T_{ev} , except for the preheat zone. Additionally, the final, adiabatic flame temperature does not change with T_{ev} , which is in the nature of the enthalpy balance.

Figure 4 shows the distributions of major species, H, O, OH, and CO, when the evaporation temperature, T_{ev} is varied from 500 K to 1500 K. It is clear that the distributions of

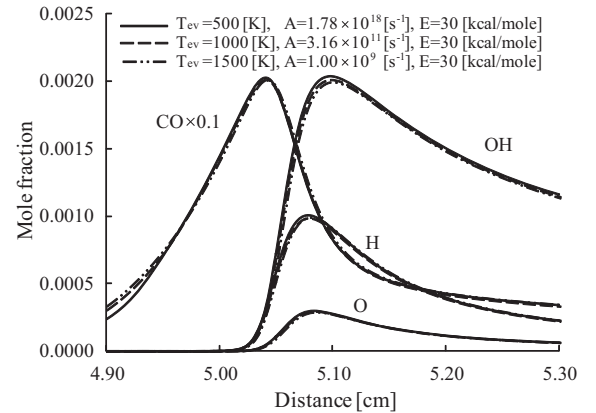


Fig. 4 Effects of T_{ev} on the major species concentrations for $\langle WM \rangle$, and $1354X_{WM} = 0.20$.

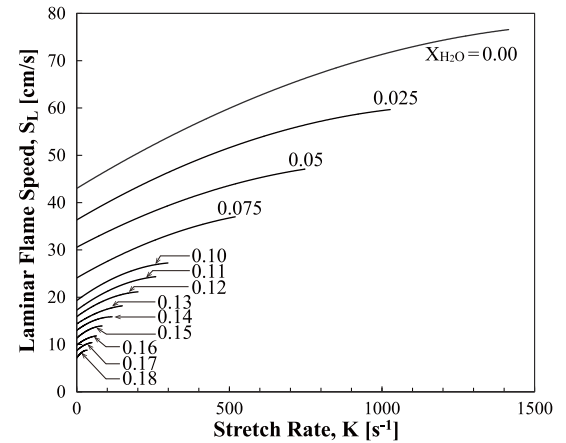


Fig. 5 Calculated laminar flame speeds with water mist for $\phi = 1.0$.

these major species are almost independent of the assumed T_{ev} , because the evaporation process of water mist only affects the preheat zone structure, and the reaction zone where the main chemical reactions occur remains unchanged even if the evaporation process in the preheat zone is varied. Hereafter, therefore, the calculation was carried out assuming $T_{ev} = 500$ K.

4.2.2 Effect of stretch rate on laminar flame speed with water mist

Numerically calculated flame speeds for the case with water mist are shown in Fig. 5 for $\phi = 1.0$. Here X_{H2O} is the water vapor mole fraction when the added water mist is completely evaporated. The terminus of each line shows the limit of extinction of the flame. Even if the water mist is added, the laminar flame speed increases with the stretch rate as without water mist. Nevertheless, at each stretch rate, the reduction of flame speed occurs with increase of

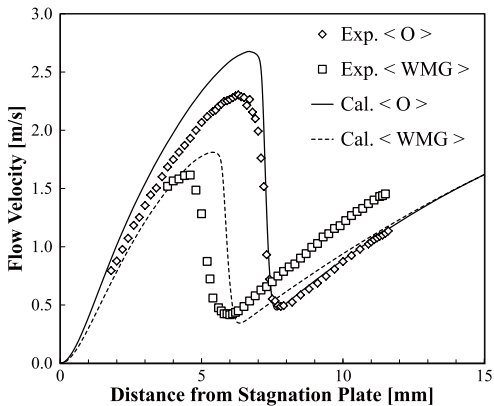


Fig. 6 Velocity profiles along the stagnation stream line with and without water mist for $\phi = 1.0$.

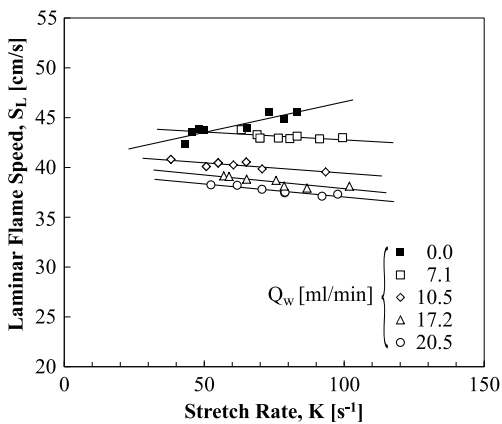


Fig. 7 Effect of stretch rate on the measured laminar flame speed with and without water mist for $\phi = 1.0$.

the amount of water mist added. Concurrently, the limit of extinguishment moves towards lower stretch rate and finally no flame can be established when X_{H2O} is larger than 0.20.

When the water mist is added to the mixture, the measured velocity profile along the stagnation stream line changes as shown in Fig. 6 in which the velocity profile without water mist is also shown for comparison. Similar velocity profiles were obtained for methane/air premixed flames with and without water mist [24]. For the case without water mist, the calculated velocity profile agrees well with experiment on the unburned gas side and in the flame zone. However, on the burned gas side, the measured velocity is significantly lower than the calculated value. In the actual flame, the burned gas is cooled by the heat loss to the water-cooled stainless steel stagnation plate, which should reduce the gas velocity. When adding the water mist, the constant velocity gradient in the upstream unburned mixture does not change. Water mist makes the apparent stagnation point move closer towards the stagnation plate than the simulation. In the flame zone, the decelerating flow field changes to accelerating one. However, the mist droplets, even if they are fine, cannot follow the flow acceleration due to the Stokes number effect as described in Re. 25. It is clear that the minimum velocity ahead of the flame zone is lower than that without water mist, suggesting that the laminar flame speed S_L decreases when the water mist is added in the unburned mixture.

Figure 7 shows the effect of stretch rate on the measured laminar flame speed for $\phi = 1.0$ with and without water mist. When adding the water mist, the dependency of flame speed on stretch rate changes from positive to negative and the laminar flame speed decreases with the stretch rate. The laminar flame speed without stretch S_L^0 obtained by extrapolating to $K = 0$ may be higher than that without water mist. This fact is inconsistent with the thermal consideration; the water mist should extract heat from the flame zone, which should result in a lower laminar flame speed as compared to that without water mist. Therefore, the apparent high flame speed at $K = 0$ is an artifact induced by the flow field inherent in the stagnation flow.

However, it should be noted that at each stretch rate, the laminar flame speed with water mist is significantly lower than that without water mist and decreases with the amount of water mist added.

In the stagnation flow configuration, the flow stream line begins to diverge after the flow emerges from the nozzle, producing radial drag forces on the mist droplets. Due to this effect, mist droplets move away from the burner axis. The inertial force is larger for large droplets and the large droplets cannot follow the radial acceleration. The equilibrium in velocities between mist droplets and gas phase is lost in the diverging flow field due to the Stokes number effect [25]. Consequently, large mist droplets are accumulated in the central portion of the flame zone. Radial acceleration is larger at higher stretch rate and more mist droplets are accumulated near the flame axis where the laminar flame speeds are determined. This flame speed reduction due to mist droplet accumulation is larger than its increase due to the flame stretch, and in total the laminar flame speed decreases with the stretch rate.

4.2.3 Effect of water vapor and water mist on laminar flame speeds

Figure 8 shows the calculated laminar flame speeds for cases of $\langle V \rangle$, $\langle R \rangle$, and $\langle WMG \rangle$. The laminar flame speed without water mist, S_L^0 , is 40.4 cm/s and is a reference. The model $\langle V \rangle$ includes the effects of dilution and the specific heat of gaseous water vapor, in which water vapor is treated as an inert gas. In the model

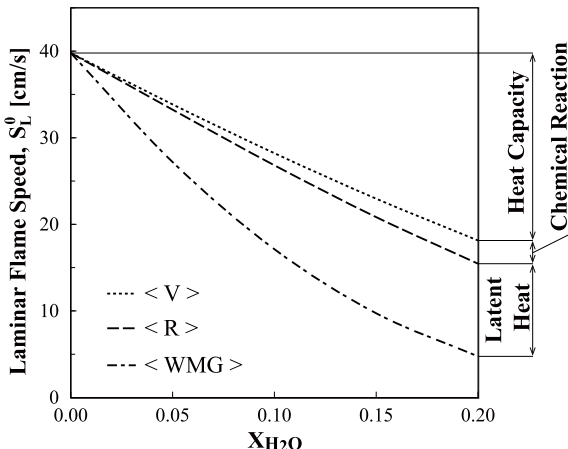


Fig. 8 Calculated laminar flame speeds for models of $\langle V \rangle$, $\langle R \rangle$ and $\langle WMG \rangle$ and $\phi = 1.0$.

$\langle R \rangle$, the added water vapor participates in the chain branching and carrying reactions containing OH radical and the chain terminating reactions including H_2O as a third body. The difference between the models $\langle V \rangle$ and $\langle R \rangle$ reflects the chemical effect of water vapor. The chemical effect is rather small, but is not negligible as compared to the dilution and thermal effects calculated by the model $\langle V \rangle$. When introducing the evaporation process of liquid water mist in the model $\langle WMG \rangle$, the laminar flame speed decreases further due to the latent heat of evaporation. Even though the water mist has no catalytic effect as bromine in Halon 1301 [26], the chaperon efficiency of water vapor is relatively high, which enhances the three-body recombination reactions terminating the global combustion reaction [27].

4.2.4 Chemical effect owing to the activity of water vapor

Figure 9 shows the logarithmic sensitivity coefficients of major reactions on the laminar flame speeds. R1 is the chain branching reaction and has the highest sensitivity to enhance the flame speed. Also the sensitivities of the chain carrying reactions R31 and R50 are positive, in opposition to R14 which is a chain terminating reaction and has negative sensitivity. With the water mist addition, R14 is enhanced and the flame speed is reduced.

Figure 10 shows the concentrations of major species which participate in the reactions of which sensitivities of flame speed are

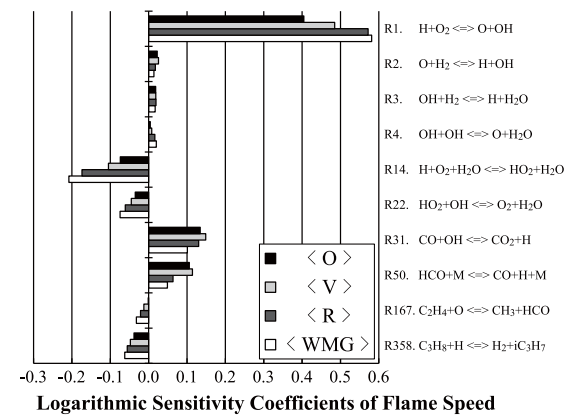


Fig. 9 Logarithmic sensitivity coefficients of major reactions on the laminar flame speeds for the models of $\langle O \rangle$, $\langle V \rangle$, $\langle R \rangle$ and $\langle WMG \rangle$ and $\phi = 1.0$, $X_{H2O} = 0.2$ for latter three.

positive. It is clear that the concentrations of H, O, and CO decrease in the order of $\langle O \rangle$, $\langle V \rangle$, $\langle R \rangle$, and $\langle WMG \rangle$. The decrease of such active radicals reduces the rates of chemical reactions of which sensitivities are positive, e.g. R1 and R31.

4.2.5 Sensitivity of chain terminating reactions including water vapor as a third body

Water vapor is known to play an important role as a third body in three-body chain terminating reactions. Figure 11 shows the logarithmic sensitivity coefficients of major reactions related to water vapor. As a reference, also shown is the sensitivity of R50 which is a chain carrying reaction with a third body. When the chemical influence of water vapor is taken into account, the sensitivities of chain terminating

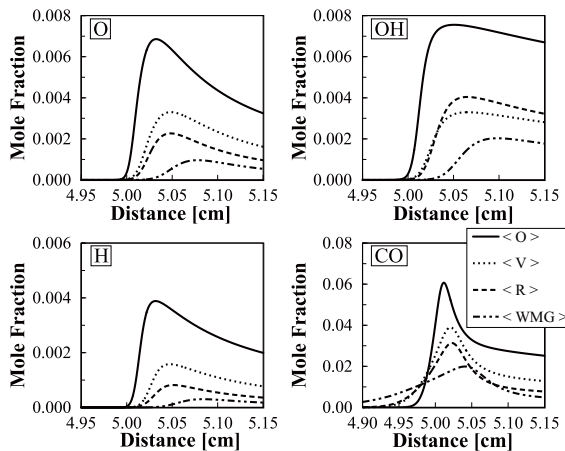


Fig. 10 Concentrations of major species participating in reactions with positive sensitivity for $\langle O \rangle$, $\langle V \rangle$, $\langle R \rangle$ and $\langle WMG \rangle$ and $\phi = 1.0$, $X_{H_2O} = 0.2$ for latter three.

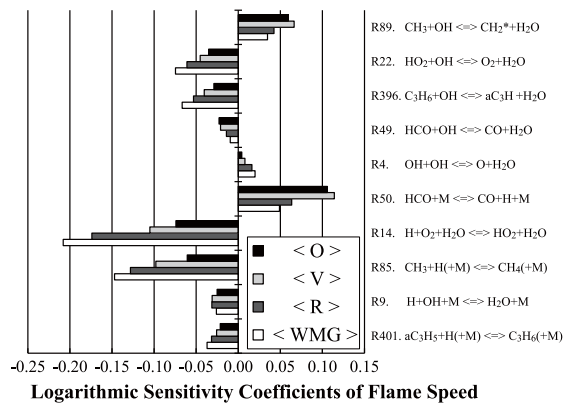


Fig. 11 Logarithmic sensitivity coefficients of major reactions related to water vapor for $\langle O \rangle$, $\langle V \rangle$, $\langle R \rangle$ and $\langle WMG \rangle$ and $\phi = 1.0$, $X_{H_2O} = 0.2$ for latter three.

reactions, R14 and R85 are considerably large negative as compared to those without water mist. The negative sensitivity increases in the order of $\langle O \rangle$, $\langle V \rangle$, $\langle R \rangle$, and $\langle WMG \rangle$ and the importance of these reactions to reduce the flame speed becomes noticeable. For both cases of gaseous water vapor and liquid water mist, the water vapor concentration is significantly higher than that without water vapor or water mist. Additionally, the chaperon efficiency of H_2O is highest among all species [27]. Therefore, these three body reactions including H_2O cause to reduce the laminar flame speeds.

4.3 Suppression Effectiveness of Typical Fire Suppressants

To compare the suppression effectiveness of water mist with typical other gaseous suppressants, numerical calculations were also carried out for N_2 , CO_2 , IG-55 (50 % N_2 , 50 % Ar) and IG-541 (52 % N_2 , 40 % Ar, 8 % CO_2).

Figure 12 shows the result as functions of X_{add} , where X_{add} is the mole fraction of an additive. Although the specific enthalpy of Ar is rather larger than N_2 on the mole base, the suppression effectiveness of N_2 is superior to IG-55, suggesting the chemical effect of N_2 . Since the specific heat of CO_2 is larger than other two, CO_2 is much more effective and consequently the effectiveness of IG-541 is nearly equal to N_2 , even though it includes Ar. It is clear that the suppression effectiveness of the water mist is larger than CO_2 . The specific heat of H_2O (vapor) on mole base is nearly equal to that of CO_2 . Therefore, the difference should be

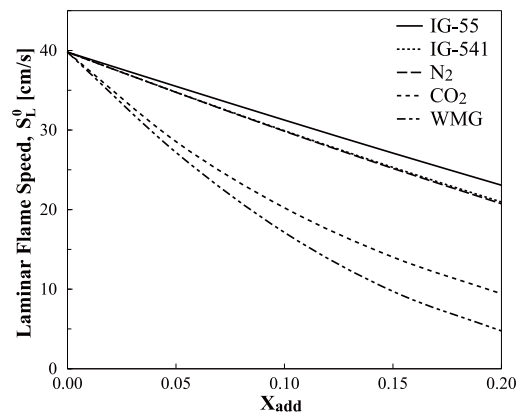


Fig. 12 Suppression effectiveness of water mist and typical fire suppressants.

attributed to the large latent heat of evaporation of water mist. Additionally, the chemical effect of water mist, discussed above, should also contribute to reduce the laminar flame speed.

5 Conclusions

The effect of water mist on laminar flame speed of propane-air premixed flame was investigated both experimentally and numerically. Experiments were performed using a single-jet-plate configuration and the OPPDIF program in CHEMKIN package was used in the numerical simulation. For the case without water mist, the laminar flame speed increases with the stretch rate towards the limit of extinction. This tendency is fairly reproducible by the numerical simulation with DLW kinetic mechanism. In the simulation with water mist, the flame speed also increases with the stretch rate, whereas the thermal, dilution and chemical effects of water mist reduce the flame speeds. However, the measured flame speed decreases with the stretch rate, because the mist droplet accumulation occurs in the diverging flow field. In addition to high heat capacity of water vapor and latent heat of evaporation of water mist, the chemical effect of water vapor also reduces the flame speed. The chemical effect is attributed in part to the decrease of active radicals and also to the enhancement of three-body chain terminating reactions. The suppression effectiveness of water mist is better than IG-55, IG-541, N₂ and CO₂.

Acknowledgements

Authors would like to thank N. Endo and A. Kageyama for their help and support in performing experiments and numerical simulations in the present study.

References

- [1] Zhang P, Zhou Y, Cao X, Cao X and Bi M. Mitigation of methane/air explosion in a closed vessel by ultrafine water fog. *Safety Science*, Vol. 62, pp 1-7, 2014.
- [2] Xu H, Li Y, Zhu P, Wang X and Zhang H. Experimental study on the mitigation via an ultra-fine water mist of methane/coal dust mixture explosions in the presence of obstacles. *J. Loss Prev. Process Ind.*, Vol. 26, pp 815-820, 2013.
- [3] Grant G, Brenton J and Drysdale D. Fire suppression by water sprays. *Prog. Energy Combust. Sci.*, Vol. 26, pp 79-130, 2000.
- [4] Liu Z and Kim A K. A review of water mist fire suppression technology: part II-application studies. *J. Fire Protec. Eng.*, Vol. 11, pp 16-42, 2001.
- [5] Mazas A N, Fiorina B, Lacoste D A and Schuller T. Effects of water vapor addition on the laminar burning velocity of oxygen-enriched methane flames. *Combust. Flame*, Vol. 158, pp 2428-2440, 2011.
- [6] Göckeler K, Albin E, Krüger O and Paschereit C O. Burning velocities of hydrogen-methane-air mixtures at highly stream-diluted conditions, *Proc. 4th Int. Conf. Jets, Wakes and Separated Flows*, pp. 1-6, 2013.
- [7] Kuznetsov M, Redlinger R, Breitung W, Grune J, Friedrich A and Ichikawa N. Laminar burning velocities of hydrogen-oxygen-steam mixtures at elevated temperatures and pressures. *Proc. Combust. Inst.*, Vol. 33, pp 895-903, 2011.
- [8] Fuss S P, Chen E F, Wang W H, Kee R J, Williams B A and Fleming J W. Inhibition of premixed methane/air flames by water mist. *Proc. Combust. Inst.*, Vol. 29, pp 361-368, 2002.
- [9] Yoshida A, Udagawa T, Momomoto Y, Naito H and Saso Y. Experimental study of suppressing effect of fine water droplets on propane/air premixed flames stabilized in the stagnation flowfield. *Fire Safety J.*, Vol. 58, pp 84-91, 2013.
- [10] Wu C K and Law C K. On the determination of laminar flame speeds for stretched flames. *Proc. Combust. Inst.*, Vol. 20, pp 1941-1949, 1984.
- [11] Law C K, Zhu D L and Yu G. Propagation and extinction of stretched premixed flames. *Proc. Combust. Inst.*, Vol. 21, pp 1419-1426, 1986.
- [12] Zhu D L, Egolfopoulos F N and Law C K. Experimental and numerical determination of laminar flame speeds of methane/(Ar, N₂, CO₂)-air mixtures as function of stoichiometry, pressure, and flame temperature. *Proc. Combust. Inst.*, Vol. 22, pp 1537-1545, 1988.
- [13] Egolfopoulos F N, Zhu D L and Law C K. Experimental and numerical determination of laminar flame speeds: mixtures of C₂-hydrocarbons with oxygen and nitrogen. *Proc. Combust. Inst.*, Vol. 23, pp 471-478, 1990.
- [14] Vagelopoulos C M, Egolfopoulos F N and Law C K. Further considerations on the determination of laminar flame speeds with the counterflow twin-flame technique. *Proc. Combust. Inst.*, Vol. 25, pp 1341-1347, 1994.

- [15] Vagelopoulos C M and Egolfopoulos F N. Direct experimental determination of laminar flame speeds. *Proc. Combust. Inst.*, Vol. 27, pp 513-519, 1998.
- [16] Linteris G T and Truett L. Inhibition of premixed methane-air flames by fluoromethanes. *Combust. Flame*, Vol. 105, pp 15-27, 1996.
- [17] Reinelt D and Linteris G T. Experimental study of the inhibition of premixed and diffusion flames by iron pentacarbonyl. *Proc. Combust. Inst.*, Vol. 26, pp 1421-1428, 1996.
- [18] Noto T, Babushok V, Hamins A and Tsang W. Inhibition effectiveness of halogenated compounds. *Combust. Flame*, Vol. 112, pp 147-160, 1998.
- [19] San Diego Mechanism Homepage, <http://web.eng.ucsd.edu/mae/groups/combustion/mechanism.html> [cited 1 December 2005].
- [20] Davis S G, Law C K and Wang H. Propene pyrolysis and oxidation kinetics in a flow reactor and laminar flames. *Combust. Flame*, Vol. 119, pp 375-399, 1999, also see <http://ignis.usc.edu/Mechanisms/C3/c3.html>.
- [21] Takahashi F and Katta V R. Extinguishment of diffusion flames around a cylinder in a coaxial air stream with dilution or water mist. *Proc. Combust. Inst.*, Vol. 32, pp 2615-2623, 2009.
- [22] Yoshida A and Yukawa A. Numerical simulation of effects of water mist on flame structure and flame speed of propane-air premixed flames, *The 9th Asia-Pacific Conference on Combustion*, 2013.
- [23] Bosschaart K J, de Goey L P H and Burgers J M. The laminar burning velocity of flames propagating in mixtures of hydrocarbons and air measured with the heat flux method. *Combust. Flame*, Vol. 136, pp 261-269, 2004.
- [24] Chen Z H, Lin T H and Sohrab S H. Combustion of liquid fuel sprays in stagnation-point-flow. *Combust. Sci. Tech.*, Vol. 60, pp 63-77, 1988.
- [25] Naito N, Uendo T, Saso Y, Kotani Y and Yoshida A. Effect of fine water droplets on extinguishment of diffusion flame stabilized in the forward stagnation region of a porous cylinder. *Proc. Combust. Inst.*, Vol. 33, pp 2563-2571, 2011.
- [26] Linteris G T, Takahashi F and Katta V R. Cup-burner flame extinguishment by CF₃Br and Br₂. *Combust. Flame*, Vol. 149, pp 91-103, 2007.
- [27] Seiser R and Seshadri K. The influence of water on extinction and ignition of hydrogen and methane flames. *Proc. Combust. Inst.*, Vol. 30, pp 407-414, 2005.

Copyright Statement

The authors confirm that they, and/or their company or organization, hold copyright on all of the original material included in this paper. The authors also confirm that they have obtained permission, from the copyright holder of any third party material included in this paper, to publish it as part of their paper. The authors confirm that they give permission, or have obtained permission from the copyright holder of this paper, for the publication and distribution of this paper as part of the ICAS 2014 proceedings or as individual off-prints from the proceedings.

Contact Author Email Address

mailto: yoshida@cck.dendai.ac.jp